Vol. 108: 1–9, 2014
doi: 10.3354/dao02698

DISEASES OF AQUATIC ORGANISMS
Dis Aquat Org

Published February 4

Cyprinid herpesvirus-2 causing mass mortality in goldfish: applying electron microscopy to histological samples for diagnostic virology

J. Lovy*, S. E. Friend

New Jersey Division of Fish & Wildlife, Office of Fish & Wildlife Health & Forensics, 605 Pequest Road, Oxford, New Jersey 07863, USA

ABSTRACT: In June 2013, a major fish kill of adult goldfish *Carassius auratus* occurred in Runnemede Lake, New Jersey, USA: an estimated 3000 to 5000 fish died within ~5 d. Necropsy of 4 moribund fish revealed severely pale gills, and histopathology showed type I and II fusion of the gills, diffuse necrosis of hematopoietic tissue in anterior and posterior kidney, and multifocal necrosis of the spleen. Within necrotic areas, pyknosis and enlarged nuclei with marginalized chromatin were observed. Cyprinid herpesvirus-2, the etiological agent for herpesviral hematopoietic necrosis disease, was confirmed in all 4 fish using PCR. We assessed the efficacy of identifying herpesviral infections (viral morphogenesis and cellular ultrastructure) using transmission electron microscopy (TEM) when applied to tissues fixed in 10% neutral buffered formalin (NBF) and tissue that was removed from paraffin blocks. Both sample types could be used to detect the virus within cells at similar concentrations. Tissues reprocessed from 10% NBF contained all the known stages of viral morphogenesis including empty capsids, capsids with an inner linear concentric density, capsids with an electron-dense core, and in the cytoplasm, mature capsids containing an envelope. Paraffin-embedded tissues showed similar stages, but viral capsids with an inner linear concentric density were rare and mature enveloped virions were not observed. In previously paraffin-embedded tissues, cellular membranes were not preserved, making identification of cell types and organelles difficult, whereas membrane preservation was good in tissues processed from 10% NBF. The results demonstrated that routinely fixed and paraffin-embedded samples can be successfully utilized to diagnose herpesviruses, and formalin-fixed tissue could be used to describe viral morphogenesis by TEM, making this a useful and reliable method for diagnostic virology when other samples are not available.

KEY WORDS: Pathology · Electron microscopy · Diagnostic virology · Mass mortality · Goldfish · *Carassius auratus* · Fish kill · New Jersey

INTRODUCTION

The cypriniviruses are double-stranded DNA herpesviruses in the family *Alloherpesviridae*, which comprises 3 species that infect cyprinid fish. These viruses are highly species-specific, with cyprinid herpesvirus-1 (CyHV-1) the cause of carp pox and cyprinid herpesvirus-3 (CyHV-3) the cause of koi herpesviral disease, both of which are limited to common carp *Cyprinus carpio* (Sano et al. 1991, Hedrick et al. 2000). Cyprinid herpesvirus-2 is the etiological agent of herpesviral hematopoietic necrosis disease (HVHN) and is found in closely related species, including goldfish *Carassius auratus* (Jeffery et al. 2007, Goodwin et al. 2009), Prussian carp *Carassius gibelio* (Daněk et al. 2012, Xu et al. 2013), and crucian carp *Carassius carassius* (Fichi et al. 2013). The CyHVs cause serious mortality in fish; carp pox pro-

*Corresponding author: jan.lovy@dep.state.nj.us

duces a papillomatous disease in carp fry (Sano et al. 1991), and koi herpesvirus can result in massive fish kills in the wild (Hedrick et al. 2000, Garver et al. 2010). Cyprinid herpesvirus-2 (CyHV-2) has a wide geographic distribution, and in North America it has been mainly associated with mortality in goldfish farms (Goodwin et al. 2006a). In mid-June 2013, a massive fish kill occurred in Runnemede Lake, Runnemede, New Jersey (NJ; USA) that attracted considerable public and media attention. The fish kill affected only goldfish and was attributed to HVHN. An intention of this study was to determine and document the presence of CyHV-2 associated with mass mortality of goldfish in this NJ lake.

In the wild, fish kills occur in a large diversity of fish species, leaving the potential for uncovering novel or emerging viruses. Diagnostic pathology is an invaluable tool for investigating fish kills because any number of environmental or infectious insults can be detected within the organs. In addition, the presence of pathogens can be linked to pathological lesions. In virology, although cell culture is considered to be the gold standard for isolating viruses, many viruses fail to replicate within cell lines due to species- and tissue-specific tropisms, leaving histopathology as the main means of detection in some instances. When histological analysis suggests a viral etiology, transmission electron microscopy (TEM) is a useful method to ultrastructurally identify the virus. Herpesviruses are the most abundant group of DNA viruses in fish, with over 14 species associated with disease in fish and nearly 30 reported herpesviruses in fish (reviewed by Hanson et al. 2011). Their species-specific nature has made them challenging to isolate and propagate in cell culture. Transmission electron microscopy has proven to be a useful method for detecting these viruses. A number of suspected disease-causing herpesviruses in fish have only been detected by TEM and have not been successfully propagated in cell culture (reviewed by Hanson et al. 2011).

In diagnostic pathology, since the majority of samples are fixed for routine histology, it is important to understand how reliably these viruses can be identified when only paraffin-embedded or formalin-fixed samples are available. For TEM, samples are optimally fixed initially in a buffered glutaraldehyde solution followed by fixation in osmium tetroxide, in order to preserve the fine cellular structures. The majority of pathology samples are preserved in 10% neutral buffered formalin (NBF) and routinely processed and embedded in paraffin wax. The ability to reprocess routinely fixed histological samples for TEM has been utilized in diagnostic pathology (Estrada et al. 2005, Graham & Orenstein 2007, Lighezan et al. 2009) and these methods have proven useful for viral diagnostics (Estrada et al. 2005) as well as for diagnostics in protozoa, fungi, and bacteria, and for examining host cell structures (Graham & Orenstein 2007). Herpesviruses are an ideal model to compare ultrastructurally because of their complex morphology containing a core, capsid, tegument, and envelope (Pellett et al. 2012). In the present study, we compared tissue and herpesviral virion ultrastructure using CyHV-2 as a model, from formalin-fixed tissue and tissue recovered from paraffin blocks reprocessed for TEM. The goal was to determine the reliability and limitations of TEM reprocessing methods for the identification of viruses.

MATERIALS AND METHODS

Fish kill at Runnemede Lake

Runnemede Lake is a ca. 1 ha lake located in Runnemede, NJ. Originally a private lake, it was formed in 1927 after a dam was built along Big Timber Creek, which flows into the Delaware River. Between 1930 and 1935, the lake was used for breeding largemouth bass and later goldfish. In 1955 the lake was purchased by the Borough of Runnemede, and in 1965 the state began stocking it with largemouth bass and sunfish. The lake is located in a residential area and is commonly used for recreational fishing.

On 21 June 2013, a fish kill was investigated at Runnemede Lake; the only species affected were goldfish, which all appeared to be in the 20 to 25 cm size range. As a response to the kill, the borough had removed approximately 950 kg of dead goldfish, estimated to be a total of 3000 to 5000 fish. Water quality analysis showed that water temperature was 22.3°C, dissolved oxygen was 6 mg l^{-1} (70% saturation), pH 7.17, and total ammonium was 0.56 mg l^{-1}. Four moribund fish were captured by wading with a dip net. Fish were euthanized with an overdose of tricaine methanesulfonate buffered with sodium bicarbonate. Necropsy was done on all fish. Bacteriological analysis included streaking kidney tissue using a 1 µl loop onto tryptic soy agar (TSA) slants; positive cultures were re-isolated onto petri dishes with TSA and identified using the API-20E system. For virology, spleen, kidney, and gill were dissected and pooled within Whirl-Pak® bags and frozen until virological analysis. For histology, gills, liver, spleen, head/trunk kidney, brain, and gastrointestinal tract were dissected, cut into 1 cm^3 pieces, and fixed into

10% NBF and processed for routine histology and stained with hematoxylin and eosin (H&E).

Virological analysis

Due to the timing of sample collection, tissue pools were frozen for 48 h and subsequently transported on ice to the NJ Department of Agriculture Animal Health Diagnostic Laboratory (Ewing, NJ). Tissue samples were homogenized, and a small sample of the homogenate was reserved for DNA extraction. The remaining homogenate was routinely processed for viral assay on epithelioma papulosum cyprini (EPC) cells and monitored for cytopathic effect (CPE) at 20°C for 7 d. In the absence of CPE, blind passage was performed, and the re-inoculated cells were observed for an additional 7 d. DNA was extracted and purified from homogenized pools of kidney, spleen, and gill with the QIAamp DNA mini kit (Qiagen) using automated sample processing in a QIAcube (Qiagen). Forward (5′-TCG GTT GGA CTC GGT TTG TG-3′) and reverse (5′-CTC GGT CTT GAT GCG TTT CTT G-3′) primers (Life Technologies) were utilized based on the protocol of Goodwin (2006). Polymerase chain reaction (PCR) was performed in 25 µl reaction volumes consisting of 5 µl of template (diluted 1:1 in nuclease-free water), 1 µl each of the forward and reverse primers (10 µM each), 12.5 µl of 2× PCR Master Mix (Invitrogen), and 5.5 µl PCR-grade water. A negative template control with nuclease-free water was used to test for contamination of reagents. PCR was performed on a Veriti® Thermocycler (Applied Biosystems) under the following conditions: initial denaturation at 95°C for 5 min; followed by 35 amplification cycles of 30 s at 95°C, annealing for 45 s at 58°C, and extension for 45 s at 72°C; with a final extension for 2 min at 72°C. PCR products were diluted 1:2 with nuclease-free water and evaluated by electrophoresis on a 2% agarose E-gel (Life Technologies) containing ethidium bromide and visualized with ultraviolet light.

Morphological comparison of tissue after formalin fixation versus recovery from paraffin

After 48 h of fixing organs in 10% NBF, a portion of all tissues was trimmed into small pieces, about 2 mm^3, fixed in 2% phosphate-buffered glutaraldehyde, and stored at 4°C for approximately 1 wk. Based on examination of H&E-stained, routinely processed histology slides of correlate samples, 2 fish were selected according to the most severe pathology in spleen and kidney, and these tissues were processed for high-resolution light microscopy (HRLM) and TEM. In order to compare the morphology and ultrastructure of samples processed from samples fixed in 10% NBF and samples embedded in paraffin wax, the correlate tissues were removed from the paraffin blocks with a razor blade. The paraffin-embedded tissues were trimmed to 2 mm^3 pieces and submersed in several changes of xylene at room temperature for a minimum of 3 h. Following deparaffinization in xylene, the samples were transferred into 100% ethanol in 2 changes for 15 min each and subsequently hydrated through a graded series of ethanol into phosphate buffer. The hydrated tissue was fixed in 2% phosphate-buffered glutaraldehyde at 4°C overnight. All tissues were processed routinely for TEM. Briefly, the tissues were washed in 0.1 M phosphate buffer, post-fixed in 1% phosphate-buffered osmium tetroxide, washed again and dehydrated through a graded series of ethanol concentrations to 100% ethanol. Samples were cleared in propylene oxide and infiltrated with Araldite 502/Embed 812 resin (Electron Microscopy Sciences) through increasing concentrations of resin in propylene oxide. Finally, tissues were embedded in pure resin and polymerized at 60°C for 24 h. Semi-thin sections (0.5 µm) were cut from each block, stained with epoxy tissue stain (Electron Microscopy Sciences), viewed with a Nikon Eclipse 600 light microscope, and photographed with a Jenoptik ProgRes Speed XT Core 3 digital camera. Areas of interest from the block were retrimmed and ultrathin sections (90 nm) were cut, mounted onto 200-mesh super grids, and stained with uranyl acetate and Sato's lead stain. Preparation of HRLM and TEM sections was done at the National Institute of Environmental Health Sciences Center at Rutgers University, and TEM scoping and imaging were done at the Division of Life Sciences, Electron Microscopy Core, Rutgers University. Measurements were made directly on electron micrographs; to compare measurements of viral capsids between formalin-fixed tissue and tissue taken from paraffin, a 1-sample *t*-test was used.

RESULTS

Fish kill at Runnemede Lake

In all 4 necropsied fish, gross findings included severely pale gills (Fig. 1a), and occasional hemorrhage occurred at the base of the fins. Internally, the

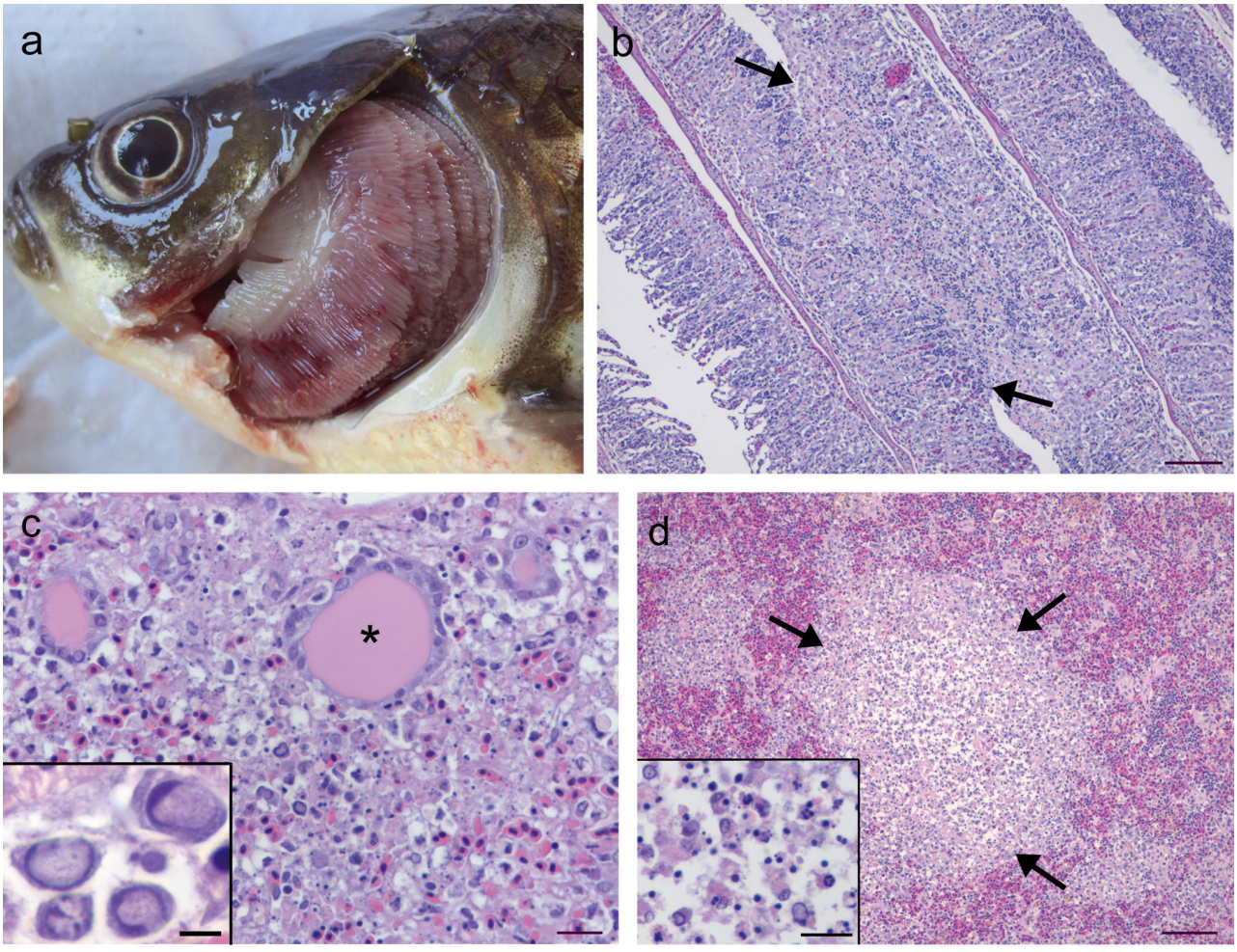

Fig. 1. *Carassius auratus*. Goldfish infected with CyHV-2, showing (a) severely pale gills, (b–d) light micrographs of routine histology sections stained with H&E. (b) Gills with type I and II (arrows) fusion with a significant loss of respiratory surface. (c) Anterior kidney with cellular necrosis, pyknotic nuclei, and dilated blood vessels containing a proteinaceous fluid (*); note the cells with enlarged nuclei with marginated chromatin (inset). (d) Spleen with multifocal necrotic foci (arrows) with necrotic cells, pyknotic nuclei, and enlarged cellular nuclei with marginated chromatin (inset). Scale bars = (b) 100 µm, (c) 20 µm, inset 5 µm, (d) 100 µm, inset 20 µm

spleen and kidney were slightly mottled, containing pale patches throughout the organs. Histopathology showed that gills had diffuse type I fusion (fusion of gill lamellae), and focal areas of type II fusion (fusion of gill filaments) in all fish (Fig. 1b). The lamellar and filament fusion in the gill was attributed to epithelial hyperplasia and an associated inflammatory infiltrate dominated by eosinophilic granule cells (EGCs). Occasionally, nuclei of cells in the gill had margination of chromatin. Diffuse and extensive necrosis with the presence of pyknotic nuclei occurred within the hematopoietic tissue in the head and trunk kidney of all fish (Fig. 1c). Additionally, many cells had marginalized chromatin with centrally pale nuclei (Fig. 1c inset). Within the head kidney, blood vessels were dilated and contained a proteinaceous fluid (Fig. 1c). In the spleen, there were multifocal areas of necrosis that contained necrotic cells, pyknotic nuclei, and enlarged centrally pale nuclei with marginated chromatin (Fig. 1d). One fish had a lesion in the brain, within the granular layer of the cerebellum, characterized by fibrous material accumulated adjacent to blood vessels, and the granular cell nuclei had marginated chromatin with centrally pale nuclei. Virological analysis demonstrated no CPE in the EPC cells inoculated with the tissue samples. PCR analysis for cyprinid herpesvirus-2 was positive in all 4 samples tested, confirmed by the presence of a 92 bp amplicon. Transmission electron microscopy of spleen and kidney confirmed the presence of herpes-

virus within the nucleus and cytoplasm of necrotic cells and cells with marginated nuclear chromatin within lesions. Bacteriology showed that 3 of the fish cultured positive for *Aeromonas sobria*.

Morphological comparison of tissue after formalin fixation versus recovery from paraffin

HRLM, 0.5 µm sections of resin-embedded tissues viewed with a light microscope had similar tissue and cellular morphology when compared between tissues processed directly from formalin or tissues processed from paraffin blocks (Fig. 2). In both processing methods, the cells were well preserved and, within the lesions of interest, cells with centrally pale nuclei and marginated chromatin were clearly evident (Fig. 2). Examining the ultrastructure with TEM, virions were clearly identifiable with both processing methods, but differences were noted in cellular and viral ultrastructure (Fig. 3). When processed directly from formalin-fixed tissue, cellular membranes were well preserved as seen by the preservation of the nuclear membrane, cisternae of rough endoplasmic reticulum, and mitochondrial membranes (Fig. 3a–d). Three types of virions were observed in the nucleus of infected cells: capsids with a central dense core (mean ± SD diameter 89.5 ± 8.23 nm, range 73–100 nm, n = 60), empty capsids (mean diameter 92.4 ±10.08 nm, range 75–100 nm, n = 10), and capsids with a concentric linear density (mean diameter 81 ± 6.32 nm, range 75–87 nm, n = 10; Fig. 3a,b). In the cytoplasm, aggregates of capsids with a dense core were clearly apparent (Fig. 3c), and capsids within host membrane-bound vesicles or capsids within a membrane-derived envelope were observed (Fig. 3d). The most notable difference in tissues processed from paraffin blocks was the loss of membrane structures (Fig. 3e–h). Ribosomes and nuclear chromatin were present in the cells, although the plasma membrane and nuclear membranes were not preserved (Fig. 3e,f,h). Within the cell cytoplasm and nucleus, herpesvirions were clearly observed at concentrations similar to that seen in tissues that were processed after formalin fixation. Similar to formalin-fixed samples, virions were observed as empty capsids (mean diameter 79.2 ± 7.2 nm, range 75–92 nm, n = 10) and capsids with a dense central core (mean diameter 84.9 ± 7.45 nm, range 75–100 nm, n = 60; Fig. 3f,g). Capsids with a concentric linear density were rarely observed, and capsids within membranous vesicles or capsids with a membrane-derived envelope were not observed in these samples. Virions with capsids surrounded by electron-dense material were observed in the cytoplasm (Fig. 3h). Comparison of the size of viral capsids with dense cores between the 2 processing methods revealed a significant difference in the size of capsids ($p = 0.00103$). The size difference was marginal with the mean capsid size of 89.5 nm in formalin-fixed tissue and 84.9 nm in tissue taken from paraffin blocks.

For diagnostic pathology, it is helpful to identify cell types and organelles using TEM; in samples that were processed after formalin fixation, there was good preservation of cellular membranes, organelles, and granules that aid in cell identification

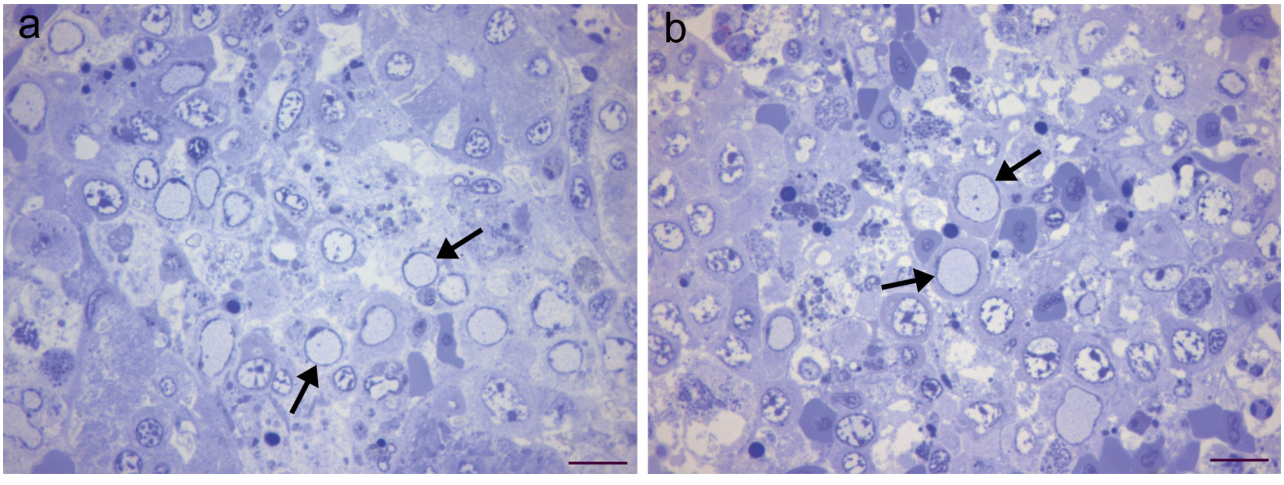

Fig. 2. *Carassius auratus*. High-resolution light microscopy stained with toluidine blue. Anterior kidney of fish infected with CyHV-2 with enlarged nuclei containing marginated chromatin (arrows), (a) processed for transmission electron microscopy (TEM) from formalin-fixed tissue, compared to (b) processed for TEM from paraffin block. Scale bars = 10 µm

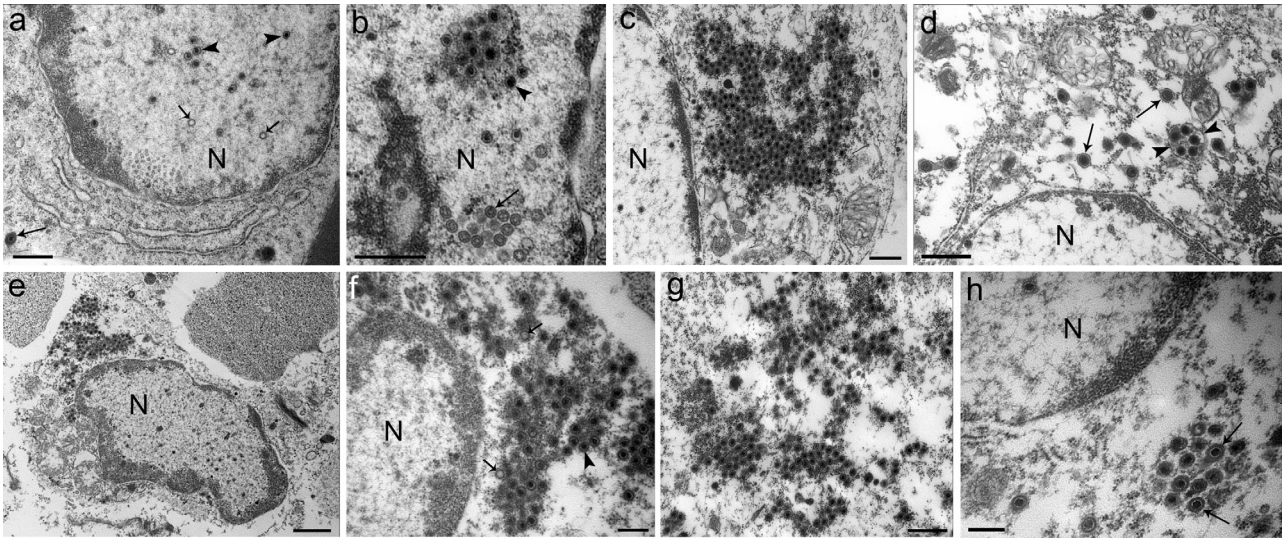

Fig. 3. *Carassius auratus*. Transmission electron microscopy (TEM) of cells infected with CyHV-2. (a–d) Tissues processed from 10% neutral buffered formalin; note the membrane preservation of the sample. (e–h) Tissues processed from paraffin blocks; note the lack of membranes. (a) Cell containing viral capsids with electron-dense cores (arrowheads) and empty viral capsids (short arrows) within the nucleus (N), and a viral capsid surrounded with electron-dense material within the cell cytoplasm (long arrow). Note the well-preserved nuclear membrane and rough endoplasmic reticulum. (b) Viral capsids with electron-dense core (arrowhead) and capsids containing a concentric linear density (arrow) in the nucleus (N). (c) Aggregate of naked viral capsids with electron-dense cores in the cytoplasm. (d) Individual enveloped mature virions (arrows) within the cytoplasm and groups of viral capsids within a membrane-bound vesicle (arrowheads). (e) Cell with an enlarged nucleus with marginated chromatin (N) containing viral capsids and cytoplasm with an aggregate of viral capsids (upper left part of the cell); note lack of plasma membrane surrounding the cell. (f) Nucleus (N) with no nuclear membrane and aggregates of viral capsids with electron-dense cores (arrowhead) and empty capsids (arrows) surrounded with electron-dense material and ribosomes. (g) Viral capsids with electron-dense cores surrounded by a washed-out cytoplasm. (h) Viral capsids in cytoplasm with electron-dense cores and capsid surrounded by electron-dense material (arrows). Scale bars = (a–d) 500 nm, (e) 1 µm, (f,h) 250 nm, (g) 500 nm

(Fig 4.a–c). Immune cells believed to be related to a dendritic cell type in cyprinids (Lovy et al. 2010) were observed in the spleen and kidney. The granules within the cells were vacuolated and contained electron-dense cores within the vacuoles. The vacuolated portion of the granule ranged from 150 to 633 nm in diameter, with a mean of 306.5 ± 174.36 nm (n = 10), and the electron-dense core ranged from 117 to 200 nm, with a mean of 136.5 ± 25.9 nm (n = 10). Within the inflammatory infiltrate of herpesviral lesions were EGCs that were both intact (Fig. 4b) and ones that were undergoing piecemeal degranulation (Fig. 4c). In tissues that were processed for TEM from paraffin blocks, it was possible to identify cell types when they had characteristic granules, although the cellular membranes were not preserved, making correct identification of cellular organelles and granules difficult (Fig. 4d,e). Additionally, the cytoplasm of the cells had a 'washed out' appearance, suggesting that some of the organelles were not entirely preserved. Within the kidney of 1 sample, gram-negative bacterial rods were observed (Fig. 4f).

DISCUSSION

This is the first documented mass mortality of wild goldfish caused by CyHV-2 in NJ. It is possible that outbreaks have occurred in the past, but have only recently been documented because of the current availability of diagnostic techniques and the residential location of this lake, making reporting more likely. Although CyHV-2 has a wide geographic range, including reports from Europe (Jeffery et al. 2007, Daněk et al. 2012, Fichi et al. 2013), Japan (Jung & Miyazaki 1995), Taiwan (Chang et al. 1999), Australia (Stephens et al. 2004), and the USA (Goodwin et al. 2006a,b), reports in the USA are rare and are usually associated with commercial goldfish operations (Goodwin 2012). Goldfish are an established invasive species in North America, originally introduced in the late 1600s (Courtenay & Stauffer 1990), and are found within many drainages throughout the state of NJ. In Runnemede Lake, the fish kill was likely initiated by increasing water temperatures combined with the high densities of goldfish in the lake. Temperature stress is also believed to be a

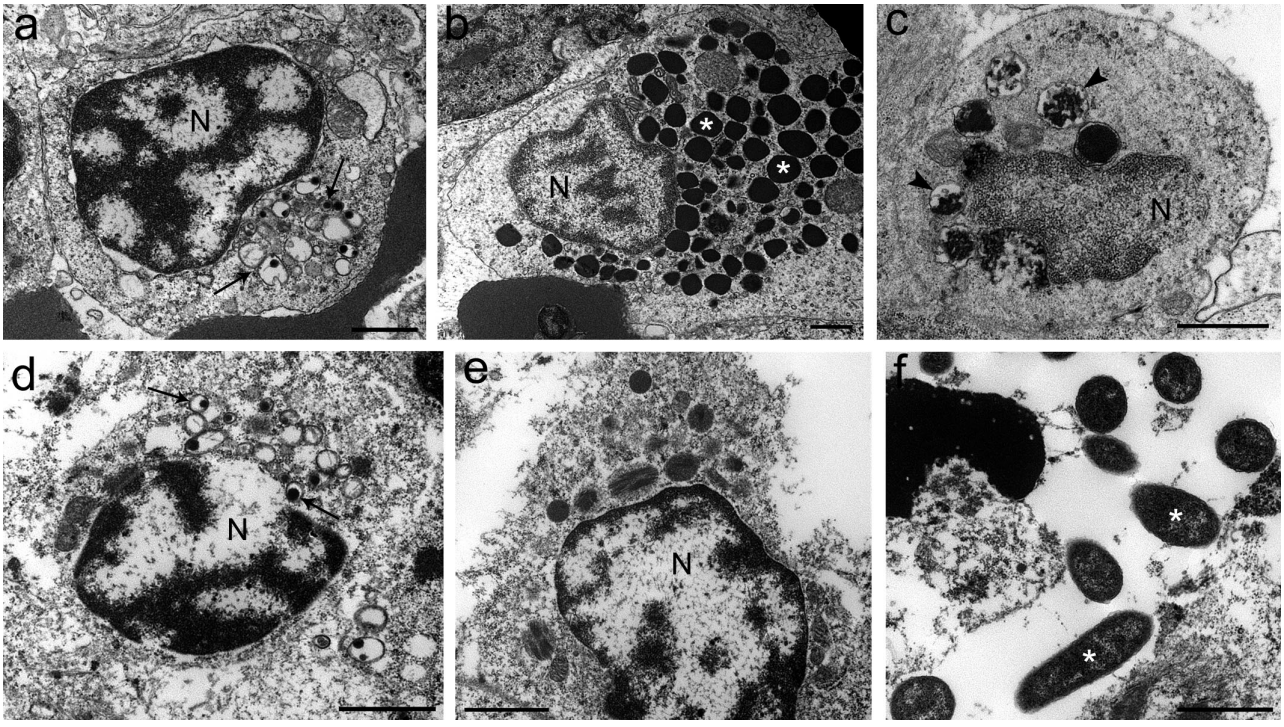

Fig. 4. *Carassius auratus*. Transmission electron microscopy (TEM) of cells reprocessed (a–c) from formalin-fixed tissue with preserved membrane structures and (d–f) from paraffin blocks lacking definition of membranes. (a) An immune cell containing vacuolated granules (arrows) often containing an electron-dense core; N: nucleus. (b) An eosinophilic granule cell with typical large electron-dense granules (*). (c) Piecemeal degranulation (arrowheads) of an eosinophilic granule cell within an inflamed and necrotic lesion. (d) Similar immune cell from (a), with typical granules (arrows) and lost definition of membrane structures and washed-out cytoplasm. (e) A granulocyte. (f) Gram-negative bacterial rods (*) within the kidney. Scale bars = 1 µm

major initiator of mass mortality of wild carp related to CyHV-3 (Garver et al. 2010). Similar to other herpesviruses, CyHVs cause latent infections that can become reactivated by temperature stress, as evidenced by CyHV-3 in common carp (St-Hilaire et al. 2005, Eide et al. 2011). It is possible that temperature stress caused recrudescence from latency to initiate this outbreak, although it is also possible that sediment and plankton are a reservoir for the virus within the ecosystem (Minamoto et al. 2011, Honjo et al. 2012). Viral DNA can persist in water for at least 3 mo following an outbreak (Minamoto et al. 2009). In the present study, goldfish were found co-infected with the bacterium *Aeromonas sobria*, although very little gross and microscopic pathology was attributed to this bacterium. It is likely that this bacterium is a secondary opportunist in an already compromised host. In mortality events in wild carp attributed to CyHV-3, other pathogens, including branchial columnaris, and *A. sobria* were found along with the virus (Garver et al. 2010), and mortality of crucian carp in Italy involved co-infections with CyHV-2 and *A. sobria* (Fichi et al. 2013).

Our study demonstrates that reprocessing formalin-fixed tissue from paraffin blocks has good diagnostic potential for identifying herpesviruses. Several forms of CyHV-2 were present in the cytoplasm and nucleus at concentrations comparable to tissues processed directly from formalin. A major advantage to this technique is that historical histology collections, where formalin-fixed tissues and fresh tissues are no longer available, may be revisited if a viral etiology is suspected. As evidenced by the ultrastructure of CyHV-2 virions and cells in this study, a major limitation in tissues processed from paraffin blocks was that membranes were not preserved in the sample, whereas the samples processed directly from formalin had well-preserved membrane structures. Cellular membrane preservation was likely lost during histology processing, specifically ethanol dehydration and xylene infiltration, prior to fixation with osmium tetroxide. The virion structures from paraffin-embedded samples also measured marginally less than samples processed directly from formalin, likely as a result of shrinkage from routine histology processing. Cyprinid herpesviral morpho-

genesis is a complex process similar to that described for mammalian herpesviruses. Numerous viral stages can be observed within the cells including 3 types of viral capsids in the nucleus and cytoplasm (Miwa et al. 2007, Wu et al. 2013). All 3 of these capsid types were observed in tissues processed from formalin-fixed tissue, whereas the capsid type containing a concentric linear density was only rarely observed in samples acquired from paraffin blocks. Similar to mammalian herpesvirus, CyHV viral capsids are believed to enter the cytoplasm through the nuclear membrane and acquire an envelope by budding into Golgi-derived cytoplasmic vesicles (Miwa et al. 2007). In the present study, mature virions within membrane envelopes were seen in tissues processed directly from formalin, but these stages were not observed in the tissues processed from paraffin blocks, due to the inadequate membrane preservation. It is clear from this study that reprocessing samples from paraffin blocks will aid in diagnosing viruses and identifying them to family or genus. Processing tissues directly from formalin provided detail in viral morphogenesis similar to descriptions from ideally TEM-fixed tissues (Miwa et al. 2007, Wu et al. 2013).

In the present study, the tissues were fixed in 2% phosphate-buffered glutaraldehyde after 48 h of formalin fixation. It is not known how the length of time in formalin prior to fixation for TEM will affect the tissues, particularly for membrane preservation, as this was not examined in the present study. It is recommended that if the use of TEM is anticipated at the onset, then tissues should be primarily fixed in 2% buffered glutaraldehyde, although due to lack of foresight for TEM analysis in a clinical setting, it is recommended to save tissue preserved in NBF. As suggested by Graham & Orenstein (2007), tissues should be replaced in a glutaraldehyde fixative as soon as TEM analysis is anticipated. Graham & Orenstein (2007) reported that tissues can remain in glutaraldehyde for years without ill effects, but generally recommended processing the tissues within 1 wk.

The identification of host cells within lesions aids in understanding the pathogenesis of disease. In the current study, immune cell types that resembled previously described Langerhans-like cells (Lovy et al. 2010) were observed in the hematopoietic tissues. These cells could be identified by their characteristic granules within the cytoplasm. With the morphology of these cells having vacuolated structures containing electron-dense cores, care must be taken to avoid confusing these structures with CyHVs which contain a capsid with an electron-dense core. The most distinguishable feature was that virions contained uniformly sized capsids and electron-dense cores, whereas Langerhans-like cell granules contained variously sized vacuoles and electron-dense cores that were generally larger in size than the virions (Fig. 4a; Lovy et al. 2010). Although host cells and granule structures were visible within cells from tissues reprocessed from paraffin blocks, the lack of membrane preservation and the 'washed out' appearance of the cytoplasm demonstrated that the cellular organelles were not reliably fixed, and cellular interpretation could not be made from tissues processed in this manner. Tissues that were processed after formalin fixation had well-preserved organelles and cellular granules. Eosinophilic granule cells, thought to be mediators of inflammation analogous to mammalian mast cells (Reite & Evensen 2006), were clearly identifiable, and evidence of piecemeal degranulation of the granules was observed within the lesions. This method of degranulation has been previously described in EGCs following activation (Vallejo & Ellis 1989, Powell et al. 1991).

Because glutaraldehyde is more effective at cross-linking proteins than formalin, it remains the preferred fixative for ultrastructural cellular observations utilizing TEM. Ideally, interpretations of cellular pathology should be made on specimens that have undergone typical TEM fixation methods. However, for the purposes of diagnostic pathology, we have demonstrated that host cell identification can be done when formalin-fixed tissues are processed for TEM, and tissues reprocessed from paraffin blocks, while lacking cellular membrane preservation, can still provide useful information in diagnostic virology. The most obvious advantage of the latter is being able to go back to paraffin-embedded tissues, allowing for analysis of past cases in histological collections. While these methods cannot replace ideal fixation and processing for TEM, they may be particularly useful in fish kill investigations when tissues were only fixed in formalin or only tissues in paraffin blocks are available.

Acknowledgements. We thank the staff at the NJ Department of Agriculture, Animal Health Diagnostic Laboratory, particularly D. DiCarlo-Emery and L. Castellano, for their assistance in bacteriological and virological examination of tissues. We also thank K. Cooper and K. Grobert at the National Institute of Environmental Health Sciences Center at Rutgers University for the use of their laboratory for sample preparation, and C. Smith for assistance in collecting fish samples for this study. This study was funded by the Federal Aid in Sport Fish Restoration Act, Project FW-69-R, and the New Jersey Hunters and Anglers Fund.

LITERATURE CITED

Chang PH, Lee SH, Chiang HC, Jong MH (1999) Epizootic of herpes-like virus infection in goldfish, *Carassius auratus* in Taiwan. Fish Pathol 34:209–210

Courtenay WR, Stauffer JR (1990) The introduced fish problem and the aquarium fish industry. J World Aquacult Soc 21:145–159

Daněk T, Kalous L, Veselý T, Krasova E and others (2012) Massive mortality of Prussian carp *Carassius gibelio* in the upper Elbe basin associated with herpesviral hematopoietic necrosis (CyHV-2). Dis Aquat Org 102:87–95

Eide KE, Miller-Morgan T, Heidel JR, Kent ML and others (2011) Investigation of koi herpesvirus latency in koi. J Virol 85:4954–4962

Estrada JC, Selim MA, Miller SE (2005) TEM of paraffin-embedded H&E stained sections for viral diagnosis (an unusual papovavirus case). Microsc Microanal 11(Suppl 2):964–965

Fichi G, Cardeti G, Cocumelli C, Vendramin N and others (2013) Detection of cyprinid herpesvirus 2 in association with an *Aeromonas sobria* infection of *Carassius carassius* (L.), in Italy. Mar 11. J Fish Dis 36:823–830

Garver KA, Al-Hussinee L, Hawley LM, Schroeder T and others (2010) Mass mortality associated with koi herpesvirus in wild common carp in Canada. J Wildl Dis 46: 1242–1251

Goodwin AE (2006) Goldfish herpesviral hematopoietic necrosis disease. In: American Fisheries Society — Fish Health Section (AFS-FHS) Blue Book: suggested procedures for the detection and identification of certain finfish and shellfish pathogens, 2012 edn. AFS-FHS, Bethesda, MD

Goodwin AE, Khoo L, LaPatra SE, Bonar C and others (2006a) Goldfish hematopoietic necrosis herpesvirus (cyprinid herpesvirus 2) in the USA: molecular confirmation of isolates from diseased fish. J Aquat Anim Health 18:11–18

Goodwin AE, Merry GE, Sadler J (2006b) Detection of the herpesviral hematopoietic necrosis disease agent (*Cyprinid herpesvirus* 2) in moribund and healthy goldfish: validation of a quantitative PCR diagnostic method. Dis Aquat Org 69:137–143

Goodwin AE, Sadler J, Merry GE, Marecaux EN (2009) Herpesviral haematopoietic necrosis virus (CyHV-2) infection: case studies from commercial goldfish farms. J Fish Dis 32:271–278

Graham L, Orenstein JM (2007) Processing tissue and cells for transmission electron microscopy in diagnostic pathology and research. Nat Protoc 2:2439–2450

Hanson L, Dishon A, Kotler M (2011) Herpesviruses that infect fish. Viruses 3:2160–2191

Hedrick RP, Gilad O, Yun S, Spangenberg JV and others (2000) A herpesvirus associated with mass mortality of juvenile and adult koi, a strain of common carp. J Aquat Anim Health 12:44–57

Honjo MN, Minamoto T, Kawabata Z (2012) Reservoirs of cyprinid herpesvirus 3 (CyHV-3) DNA in sediments of natural lakes and ponds. Vet Microbiol 155:183–190

Jeffery KR, Bateman K, Bayley A, Feist SW and others (2007) Isolation of a cyprinid herpesvirus 2 from goldfish, *Carassius auratus* (L.), in the UK. J Fish Dis 30:649–656

Jung SJ, Miyazaki T (1995) Herpesviral haematopoietic necrosis of goldfish, *Carassius auratus* (L.). J Fish Dis 18: 211–220

Lighezan R, Baderca F, Alexa A, Lacovliev M, Bonte D, Murarescu ED, Nebunu A (2009) The value of the reprocessing method of paraffin-embedded biopsies for transmission electron microscopy. Rom J Morphol Embryol 50: 613–617

Lovy J, Wright GM, Speare DJ, Tyml T, Dykova I (2010) Comparative ultrastructure of Langerhans-like cells in spleens of ray-finned fishes (Actinopterygii). J Morphol 271:1229–1239

Minamoto T, Honjo MN, Uchii K, Yamanaka H and others (2009) Detection of cyprinid herpesvirus 3 DNA in river water during and after an outbreak. Vet Microbiol 135: 261–266

Minamoto T, Honjo MN, Yamanaka H, Tanaka N, Itayama T, Kawabata Z (2011) Detection of cyprinid herpesvirus-3 DNA in lake plankton. Res Vet Sci 90:530–532

Miwa S, Ito T, Sano M (2007) Morphogenesis of koi herpesvirus observed by electron microscopy. J Fish Dis 30: 715–722

Pellett PE, Davison AJ, Eberle R, Ehlers B and others (2012) Herpesvirales. In: King AMQ, Adams MJ, Carstens EB, Lefkowitz EJ (eds) Virus taxonomy. Ninth Report of the International Committee on Taxonomy of Viruses. Elsevier Academic Press, San Diego, CA, p 99–107

Powell MD, Wright GM, Burka JF (1991) Degranulation of eosinophilic granule cells induced by capsaicin and substance P in the intestine of the rainbow trout (*Oncorhynchus mykiss* Walbaum). Cell Tissue Res 266:469–474

Reite OB, Evensen O (2006) Inflammatory cells of teleostean fish: a review focusing on mast cell/eosinophilic granule cells and rodlet cells. Fish Shellfish Immunol 20:192–208

Sano T, Morita N, Shima N, Akimoto M (1991) *Herpesvirus cyprini*: lethality and oncogenicity. J Fish Dis 14:533–543

St-Hilaire S, Beevers N, Way K, Le Deuff RM, Martin P, Joiner C (2005) Reactivation of koi herpesvirus infections in common carp *Cyprinus carpio.* Dis Aquat Org 67: 15–23

Stephens FJ, Raidal SR, Jones B (2004) Haematopoietic necrosis in a goldfish (*Carassius auratus*) associated with an agent morphologically similar to herpesvirus. Aust Vet J 82:167–169

Vallejo AN, Ellis AE (1989) Ultrastructural study of the response of eosinophil granule cells to *Aeromonas salmonicida* extracellular products and histamine liberators in rainbow trout *Salmo gairdneri* Richardson. Dev Comp Immunol 13:133–148

Wu T, Ding Z, Ren M, An L and others (2013) The histo- and ultra-pathological studies on a fatal disease of Prussian carp (*Carassius gibelio*) in mainland China associated with cyprinid herpesvirus 2 (CyHV-2). Aquaculture 412–413:8–13

Xu J, Zeng L, Zhang H, Zhou Y, Ma J, Fan Y (2013) Cyprinid herpesvirus 2 infection emerged in cultured gibel carp, *Carassius auratus gibelio* in China. Vet Microbiol 166: 138–144

Editorial responsibility: Mark Crane, Geelong, Victoria, Australia

Submitted: October 2, 2013; Accepted: November 19, 2013
Proofs received from author(s): January 10, 2014